Electronic Supplementary Material (ESI) for Materials Chemistry Frontiers.

Supplementary Information

2D/2D graphitic carbon nitride/N-doped graphene hybrid as an effective polysulfide mediator in lithium–sulfur batteries

Junsheng Ma, [a] Mingpeng Yu,*[a] Huanyu Ye, [a] Hongquan Song,*[a] Dongxue Wang, [a] Yanting Zhao, [a] Wei Gong [c] and Hong Qiu [a]

[a] *Beijing Key Laboratory for Magneto-Photoelectrical Composite and Interface Science, School of Mathematics and Physics, Department of Physics, University of Science and Technology Beijing, Beijing 100083, People's Republic of China*

[b] *College of Physics and Telecommunication Engineering, Zhoukou Normal University, Zhoukou 466001, People's Republic of China*

[c] *School of Engineering, The University of Tokyo, Bunkyo-ku, Tokyo 113-8656, Japan*

E-mail: * yum@ustb.edu.cn * shq.zknu@foxmail.com

1. Experimental Section

Materials Preparation

All reagents were of analytical grade and purchased from commercial sources, and used without further purification.

Preparation of NG: Graphene oxide (GO) were prepared from graphite powder by the modified Hummers' method *via* a low-temperature fabrication process. [S1] The as-obtained graphene sheets exhibit better conductivity because of structural integrity with lower defect density. [S2] NG was synthesized according to the procedure in our previous report. [S3] Briefly, amphiphilic triblock copolymer P123 (0.2 g) was added into the GO aqueous dispersion (200 mL, 2 mg mL^{-1}) under vigorous stirring to dissolve. Subsequently, melamine (1.0 g) was slowly added and the mixed solution was refluxed in oil bath at 90 °C for 3 h. Then, the mixture was washed with ethanol and deionized water, followed by using vacuum freeze-drying method to remove water in the mixture. Finally, the as-obtained product was heated in a tube furnace at 800 °C for 2 hours under N_2 flow with a ramping rate 3 °C min^{-1} to obtain NG powder.

Preparation of PCN and other control samples: The raw melamine was first pretreated by the hydrothermal treatment according to a previous report. [S4] In a typical synthesis, 4.28 g of urea and 3 g of melamine (molar ratio of urea:melamine = 3:1) was added in 50 mL deionized water under magnetic stirring at room temperature. After stirring for 30 min, the resulting suspension was then transferred into a 100 mL Teflon-lined stainless steel autoclave and heated at 180 °C for 24 hours in an oven. After cooling to room temperature, the precipitate was collected by vacuum filtration, washed with deionized water, and then dried at 60 °C overnight. Afterwards, the resultant product was calcined in a corundum crucible with a cover at 600 °C under air for 2 hours with a ramp rate of 2.3 °C min^{-1} to obtain PCN. The bulk g-C_3N_4 was synthesized *via* calcination of raw melamine (5 g) in a corundum crucible with a cover at 600 °C under air for 2 hours with a ramp rate of 2.3 °C min^{-1}. The pure g-C_3N_4 was synthesized *via* the same manner with PCN, except that pre-hydrothermal treatment of melamine without adding urea.

Preparation of PCN/CN hybrids: Firstly, the raw melamine was pretreated by employing the same way as that of PCN. Secondly, the pretreated melamine powder was mixed with NG powder in a certain mass ratio by fully ball-milling at 300 rpm (revolutions per minute) for 2 hours. Finally, the as-obtained product was processed by a calcination treatment in a corundum crucible with a cover at 600 °C under air for 2 hours with a ramp rate of 2.3 °C min^{-1} to PCN/CN hybrids. The obtained hybrids are denoted as PCN/NG-A, PCN/NG-B and PCN/NG-C, corresponding to the mass ratio (pretreated melamine to NG) of 5:1, 1:1 and 1:5, respectively.

Preparation of sulfur-based composites: PCN/NG/S and NG/S composites were prepared through a simple melting diffusion method. Generally, sublimed sulfur and host materials with a mass ratio of 7:3 were mixed by ball-milling at 200 rpm for 1 hour. Then, the mixtures were treated at 155 °C for 12 hours in an Ar-filled autoclave to enable sulfur impregnation into host material frameworks via capillary action. The as-obtained sulfur-based composites were further ball milled and sieved with a 200 mesh filter for use.

Materials Characterization

The morphology and microstructure of the samples were characterized by field-emission scanning electron microscopy (FE-SEM, Zeiss Supra 55) and transmission electron microscopy (TEM, JEOL JEM-2200FS) equipped with an energy-dispersive X-ray spectroscope (EDS) detector. Nitrogen adsorption-desorption measurements were determined from an automated adsorption system (Micromeritics ASAP 2460) in a N_2 atmosphere at 77 K. X-ray diffraction (XRD) patterns were collected on a X-ray diffractometer (Rigaku SmartLab) with Cu K_α radiation ($\lambda = 1.5406$ Å) as X-ray source. X-ray photoelectron spectra (XPS) were carried out using a X-ray photoelectron spectrometer (PHI-5000 VersaProbe) with monochromatic Al K_α radiation. The scanning TEM (STEM) image and corresponding EDS mapping were also recorded through the JEOL JEM-2200FS TEM. Thermogravimetric analysis (TGA) was conducted on a PerkinElmer thermogravimetric analyzer under nitrogen gas atmosphere at a heating rate of 10 °C min^{-1} from 0 to 500 °C.

Lithium Polysulfides Adsorption Tests:

We adopted Li_2S_6 as the representative of lithium polysulfides (LiPSs) to simplify the experiments. The Li_2S_6 solution was prepared by chemically reacting stoichiometric amounts of Li_2S and sublimed sulfur with a molar ratio of 1:5, which were added into 1 M lithium bis(trifluoromethanesulfony)limide (LiTFSI) in 1,3-dioxolane (DOL) and 1,2-dimethoxyethane (DME) solvents (1:1 by volume) solution with 2 wt.% $LiNO_3$ and then vigorously stirring at 70 °C for 48 hours in an argon-filled glove box (MBraun UNIlab). Before the LiPSs adsorption test, all the samples of the same quantity (10 mg) were dried under vacuum at 70 °C for 12 hours. Then, the samples were dispersed into the above-prepared Li_2S_6 solution (5 mL, 1×10^{-3} M) and gently stirred for 10 min. After that, the turbid solution were kept standing for 24 hours to observe the color change. All testing process above was performed in an argon-filled glove box. The supernatant of above solution were used for testing adsorption ability of samples by an ultraviolet-visible (UV-Vis) absorption spectrophotometer (PerkinElmer Lambda 950).

Cell Assembly and Electrochemical Measurements

The electrochemical performance was evaluated by employing CR2032 coin-type cells, which were assembled in an argon-filled glove box with the oxygen and water content below 1 ppm. The cathodes were prepared by fully blending 80% sulfur-based composites, 10% conductive additives (Super P), and 10% polyvinylidenedifluoride (PVDF) binder in an appropriate amount of N-methyl-2-pyrrolidone (NMP) at room temperature. Then, the obtained slurry was uniformly pasted onto the carbon-coated aluminum foil using a doctor blade and dried at 60°C in a vacuum oven overnight to remove the solven, followed by cutting into round disks with a diameter of 8 mm. The average sulfur loadings of cathodes was about 1.5 mg cm^{-2}. The lithium metal was used as the counter and reference electrodes. A Celgard 2400 polypropylene membrane was employed as the separator. 1 M LiTFSI in a mixed solvent DOL and DME (v/v = 1/1) with 2 wt.% $LiNO_3$ was chosen as the electrolyte of the cells. The electrolyte/sulfur ratio in the cell was fixed at 30 μL mg^{-1}. The cells were held at open circuit at room temperature for 12 hours before the electrochemical tests, and the specific capacities of the batteries were calculated based on the mass of sulfur loading. Cyclic voltammograms (CV, 1.7-2.8 V vs. Li^+/Li, 0.05 mV s^{-1}) and electrochemical impedance spectroscopy (EIS, 0.1 Hz-100 kHz, 5 mV) measurements were performed on an electrochemical workstation (Chenhua CHI 760D). Galvanostatic charging/discharging experiments were measured by using a multichannel battery testing system (LANHE CT-2001A) at different discharge/charge current rates in a potential window of 1.7-2.8 V (vs. Li^+/Li) .

Density functional theory calculations

All calculations were carried out in this study with the DMol3 program package. [S5] The exchange and correlation potential was calculated by using the generalized gradient approximation of Perdew et al. [S6] The valence electron functions were expanded into a set of numerical atomic orbitals by a double-numerical basis with polarization functions. The convergence criterion of optimal geometry which were based on the energy, force, and displacement convergence are 1×10^{-5} Hartree, 2×10^{-3} Hartree, and 5×10^{-4} nm, respectively. Considering the calculated accuracy and efficiency, we modelled the monolayer gC_3N_4 structure type by a periodic 2x2 unit cell as the platform for the adsorption of Li_2S and Li_2S_4 molecules. The lattice constants of supercell (containing vacuum layer in vertical direction) are larger than 1.4 nm, which is large enough to eliminate the interaction between the layer and its images.

The adsorption energy (E_{ads}) of lithium polysulfides on the gC_3N_4 is defined as

$$E_{ads} = E_{gC_3N_4} + E_{Li_2S_x} - E_{gC_3N_4+Li_2S_x}$$

where $E_{gC_3N_4}$, $E_{Li_2S_x}$, and $E_{gC_3N_4+Li_2S_x}$ represent the ground-state energies of the gC_3N_4, lithium polysulfide, and gC_3N_4 adsorbed with polysulfide respectively. A larger positive value is indicative of greater binding ability. The linear or quadratic synchronous transit (LST/QST) method [S7] combined with conjugate gradient refinements was adopted for the transition state (TS) search that was implemented in the DMol3 package [S8, S9].

2. Supplementary tables

Table S1. Brunauer–Emmett–Teller (BET) surface areas and pore parameters of the samples.

Sample	BET Surface Area ($m^2\ g^{-1}$)	Pore Volume ($cm^3\ g^{-1}$)	Average Pore Size (nm)
PCN	122.06	0.81	24.2
NG	85.04	0.23	8.21
PCN/NG	102.83	0.46	24.3
CN/NG/S	0.27	0.03	——

Table S2. The elements and corresponding content (atom%) of PCN, NG and PCN/NG hybrid.

Sample	C (atom%)	N (atom%)	O (atom%)
PCN	40.33	56.91	2.76
PCN/NG	79.99	18.76	1.25
NG	89.34	3.8	5.18

Table S3. Summary on adsorption energies E_{abs} of Li_2S_x (x = 1 and 4) molecules on PCN and graphene surfaces.

Substrate	**adsorption energies E_{ads} (eV)**	
	Li_2S	Li_2S_4
PCN	−1.24	−0.89
Graphene	−0.33	−0.22

3. Supplementary figures

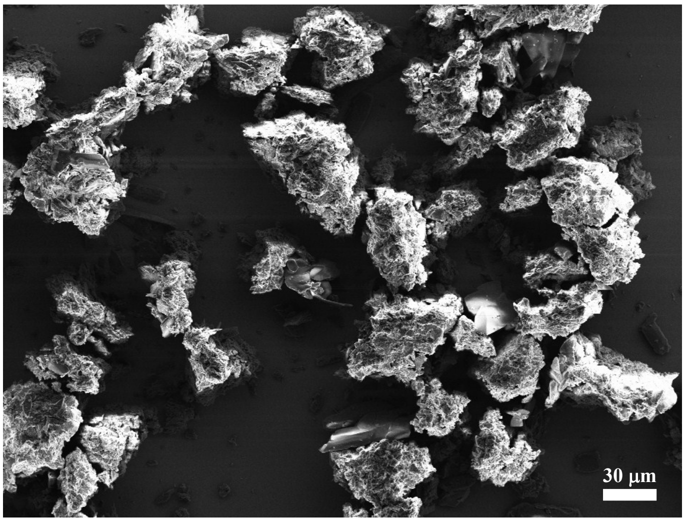

Figure S1. SEM image of bulk g-C_3N_4.

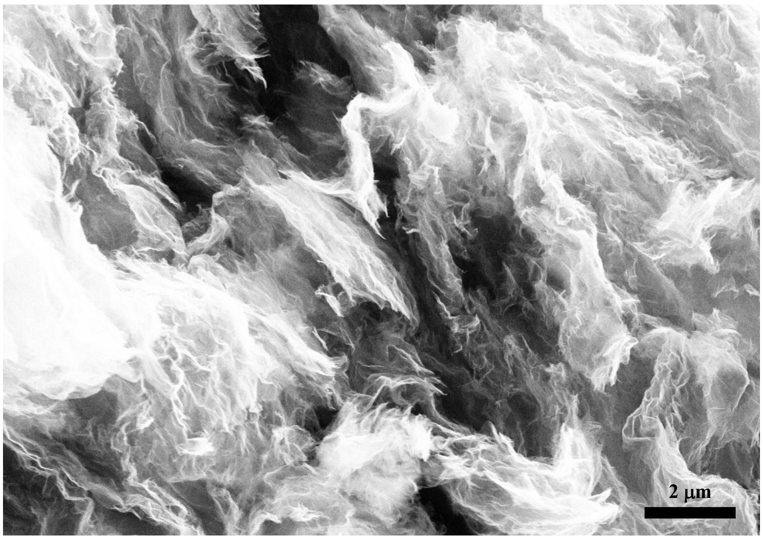

Figure S2. SEM image of NG.

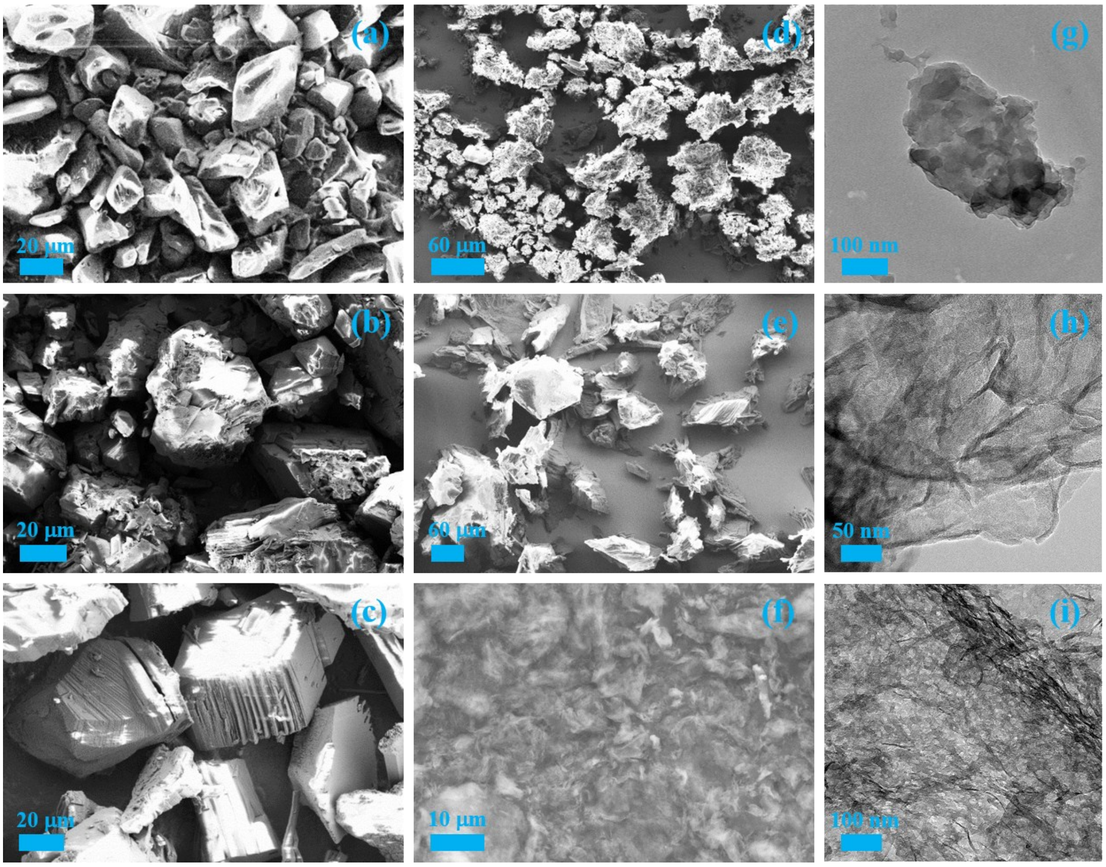

Figure S3. SEM images of (a) raw melamine (monoclinic-phase), (b) orthorhombic-phase melamine (pretreated with a hydrothermal process) and (c) orthorhombic-phase melamine (pretreated with a hydrothermal process in the presence of urea). SEM and TEM images of (d, g) bulk g-C_3N_4 (direct calcination of raw melamine), (e, h) pure g-C_3N_4 (calcination of orthorhombic-phase melamine pretreated with a hydrothermal process) and (f, i) PCN (calcination of orthorhombic-phase melamine pretreated with a hydrothermal process in the presence of urea), respectively.

Raw melamine shows spindle-shape morphology (**Figure S3a**), but the pretreated melamine presents a layered particle shape with rough surfaces after hydrothermal pretreatment (**Figure S3b, c**). Moreover, the crystal phase of melamine transformed from the monoclinic phase to the orthorhombic phase (JCPDS Card No.90-1890), as confirmed by XRD pattern of (**Figure S4**). By further calcination process, PCN (with addition of urea) formed the ultrathin g-C_3N_4 enriched with meosopores (**Figure S3f, i**). However, the bulk g-C_3N_4 derived from raw melamine shows typical aggregates (**Figure S3d, g**), and pure g-C_3N_4 (without addition of urea) shows a sheet-like morphology with a smooth surface (**Figure S3e, h**). This illustrates that the hydrothermal pretreatment in the presence of urea is a key factor for the formation of porous g-C_3N_4 nanosheets.

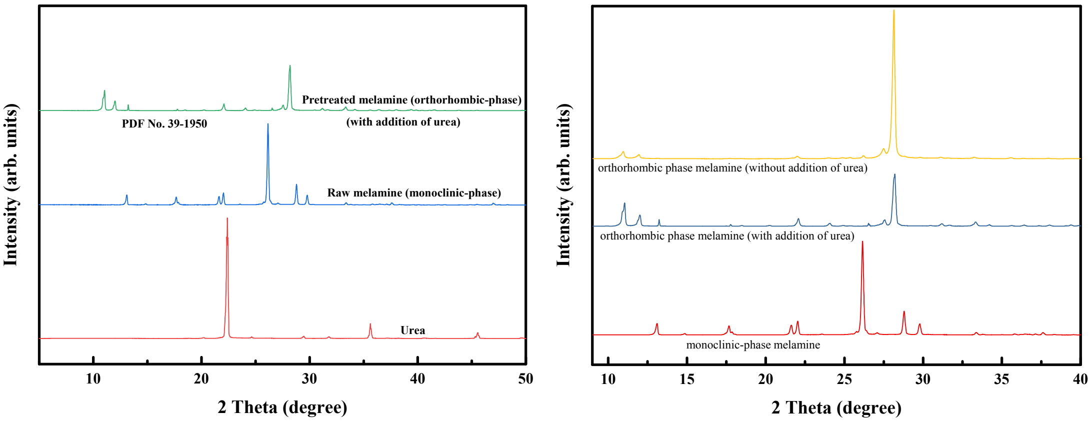

Figure S4. XRD patterns of raw melamine (monoclinic-phase), orthorhombic-phase melamine (pretreated with a hydrothermal process) and orthorhombic-phase melamine (pretreated with a hydrothermal process in the presence of urea).

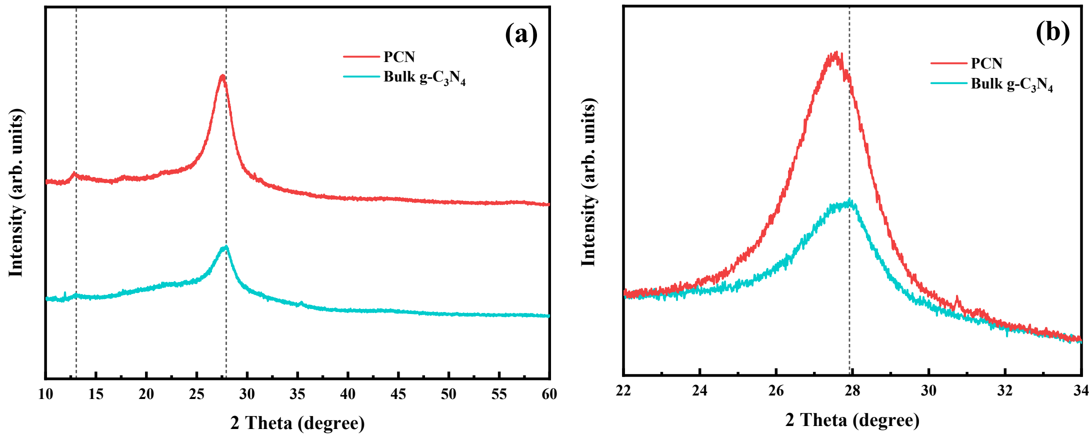

Figure S5. (a, b) XRD patterns of PCN and bulk g-C_3N_4.

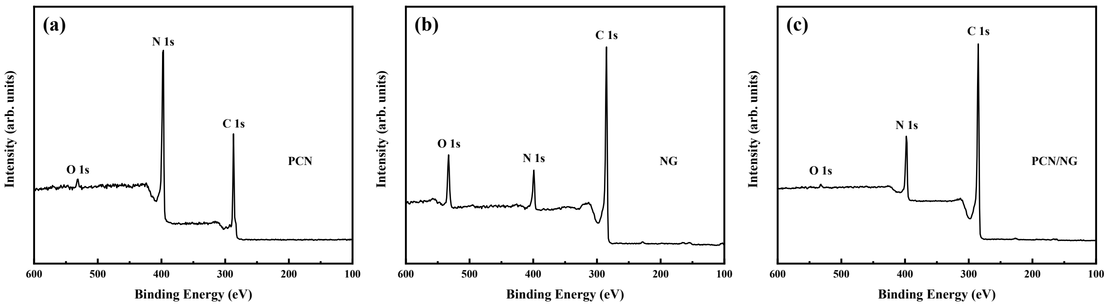

Figure S6. XPS survey scan spectra of the (a) PCN, (b) NG and (c) PCN/NG hybrid.

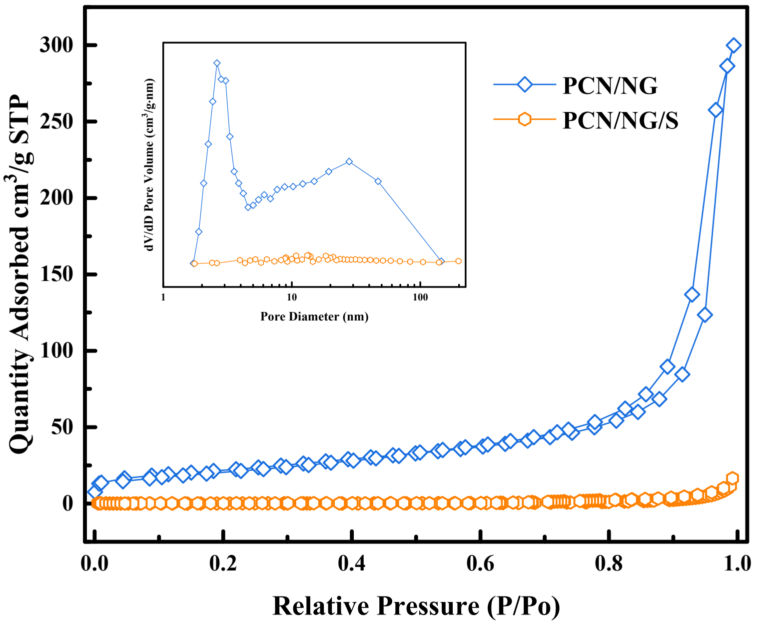

Figure S7. Nitrogen adsorption–desorption isotherm curves of PCN/NG hybrid and PCN/NG/S composite, and the corresponding pore-size distributions (inset)

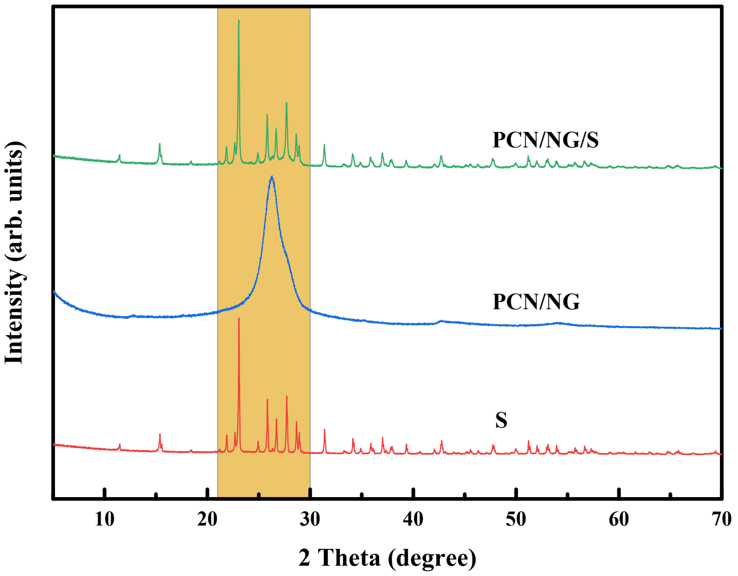

Figure S8. XRD patterns of PCN/NG/S composite, PCN/NG hybrid and sulfur.

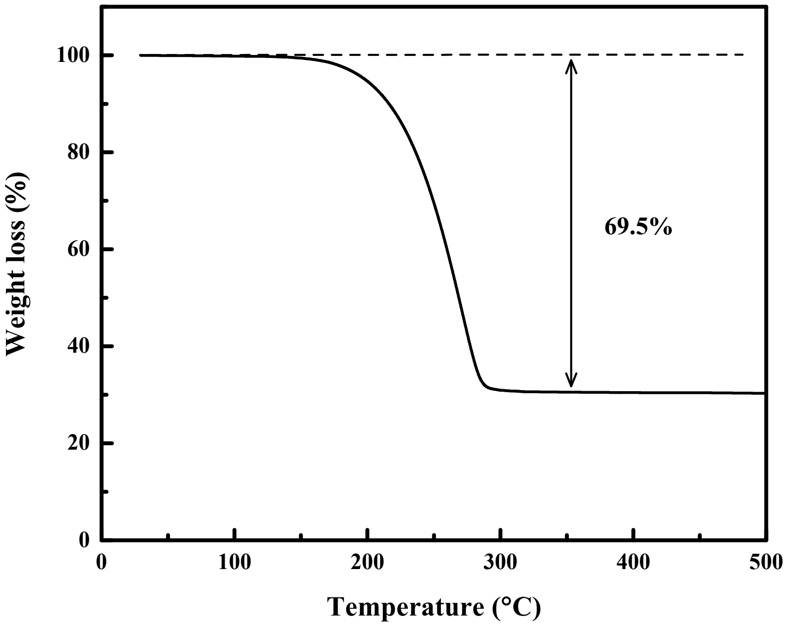

Figure S9. Thermal gravity analysis (TGA) curve of PCN/NG/S composite.

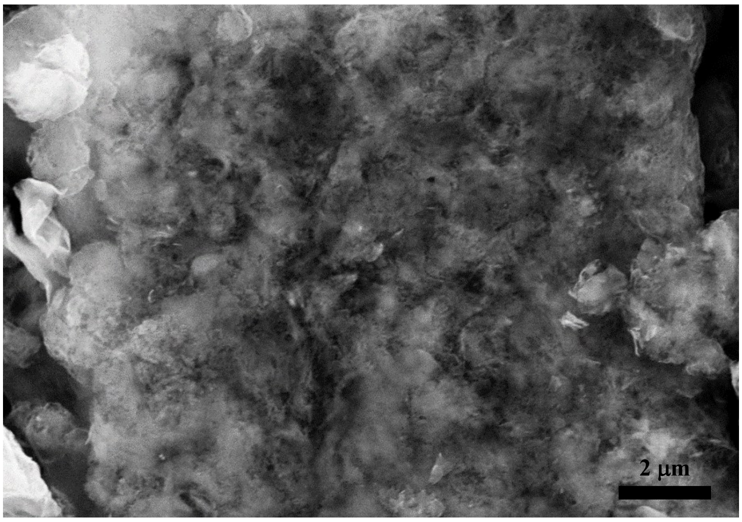

Figure S10. SEM image of PCN/NG/S composite.

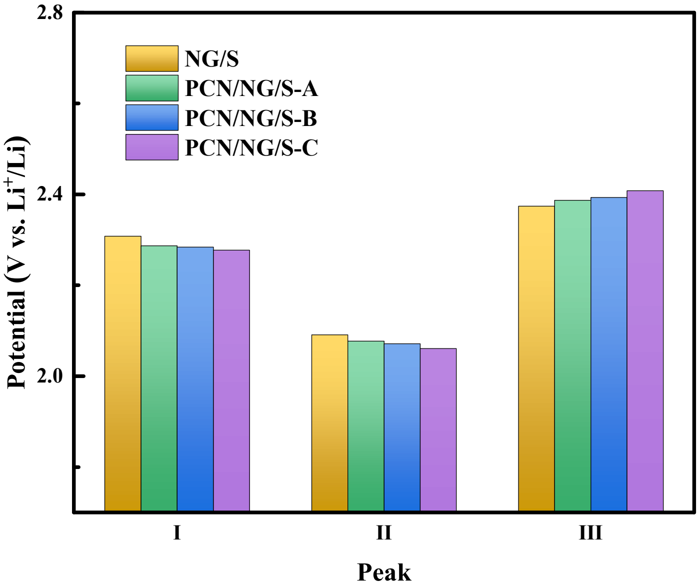

Figure S11. Peak potentials of the NG/S, PCN/NG/S-A, PCN/NG/S-B and PCN/NG/S-C cathodes.

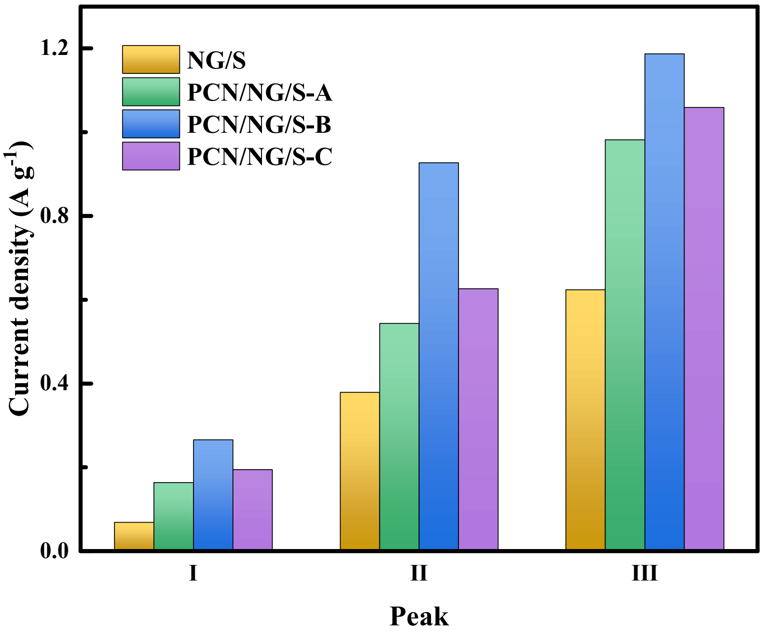

Figure S12. Peak current densities of the NG/S, PCN/NG/S-A, PCN/NG/S-B and PCN/NG/S-C cathodes.

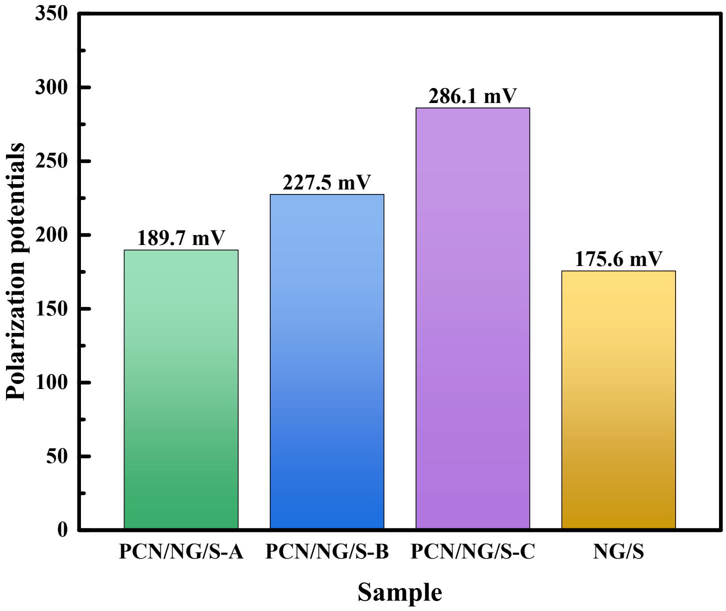

Figure S13. Polarization potentials of the 20th cycle based on PCN/NG/S-A, PCN/NG/S-B, PCN/NG/S-C and NG/S cathodes at 0.2 C.

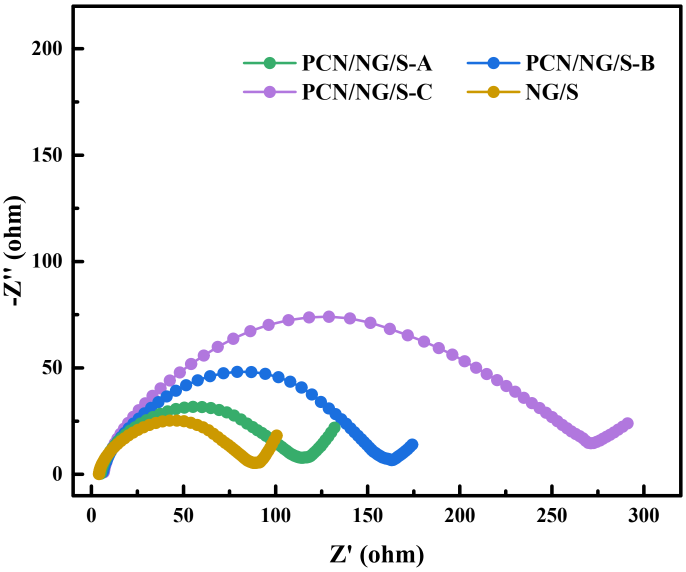

Figure S14. EIS profiles the PCN/NG/S-A, PCN/NG/S-B, PCN/NG/S-C and NG/S cathodes.

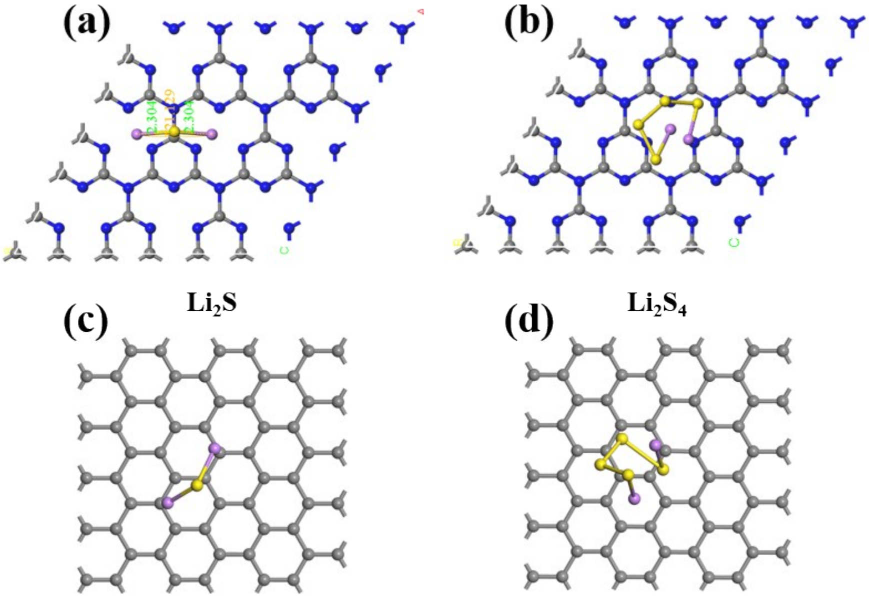

Figure S15. Optimal configurations (top view) of Li_2S_x (x =1 and 4) molecules adsorbed on (a, b) PCN and (c, d) graphene surfaces.

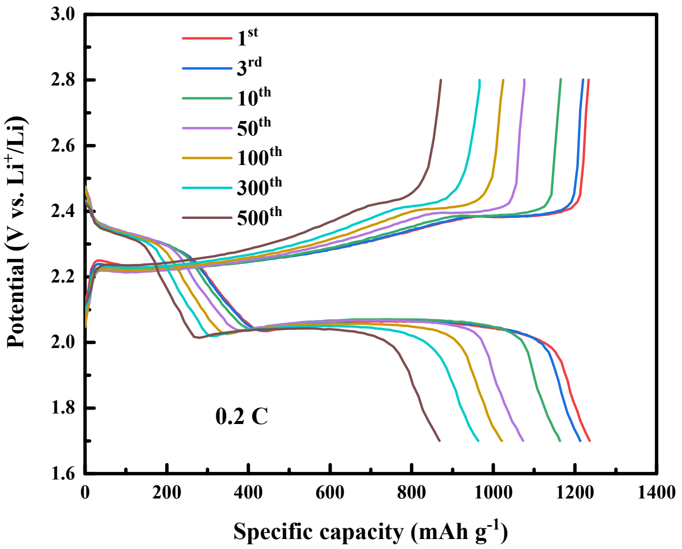

Figure S16. Galvanostatic charge/discharge profiles of PCN/NG/S-B cathodes at 0.2 C for 500 cycles.

References

[S1] S. Eigler, M. Enzelberger-Heim, S. Grimm, P. Hofmann, W. Kroener, A. Geworski, C. Dotzer, M. Röckert, J. Xiao, C. Papp, O. Lytken, H.-P. Steinrück, P. Müller and A. Hirsch, *Adv. Mater.*, 2013, **25**, 3583-3587.

[S2] M. Zhang, Y. Wang, L. Huang, Z. Xu, C. Li and G. Shi, *Adv. Mater.*, 2015, **27**, 6708.

[S3] M. Yu, J. Ma, M. Xie, H. Song, F. Tian, S. Xu, Y. Zhou, B. Li, D. Wu, H. Qiu and R. Wang, *Adv. Energy Mater.*, 2017, **7**, 1602347.

[S4] N. Tian, Y. H. Zhang, X. W. Li, K. Xiao, X. Du, F. Dong, G. I. N. Waterhouse, T. R. Zhang and H. W. Huang, *Nano Energy*, 2017, **38**, 72-81.

[S5] B. Delley, *J. Chem. Phys.*, 2000, **113**, 7756.

[S6] J. P. Perdew, K. Burke and M. Ernzerhof, *Phys. Rev. Lett.*, 1996, **77**, 3865.

[S7] T. A. Halgren and W. N. Lipscomb, *Chem. Phys. Lett.*, 1977, **49**, 225-232.

[S8] B. Delley, *J. Chem. Phys.*, 1990, **92**, 508-517.

[S9] B. Delley, *J. Chem. Phys.*, 2000, **113**, 7756-7764.